Supporting Information

Carbon Quantum Dot-Induced MnO_2 Nanowire Formation and Construction of a Binder-Free Flexible Membrane with Excellent Superhydrophilicity and Enhanced Supercapacitor Performance

Haipeng Lv,[†] Xiujiao Gao,[†] Qunjie Xu,[†] Haimei Liu,[*,†] Yong-Gang Wang,[*,§] Yongyao Xia[§]

[†]Shanghai Key Laboratory of Materials Protection and Advanced Materials in Electric Power, College of Environmental and Chemical Engineering, Shanghai University of Electric Power, Shanghai 200090, China

[§]Department of Chemistry and Shanghai Key Laboratory of Molecular Catalysis and Innovative Materials, Institute of New Energy, Fudan University, Shanghai 200433, China.

Corresponding Authors

*(H. L.) Email: liuhm@shiep.edu.cn.

*(Y. W.) Email: ygwang@fudan.edu.cn.

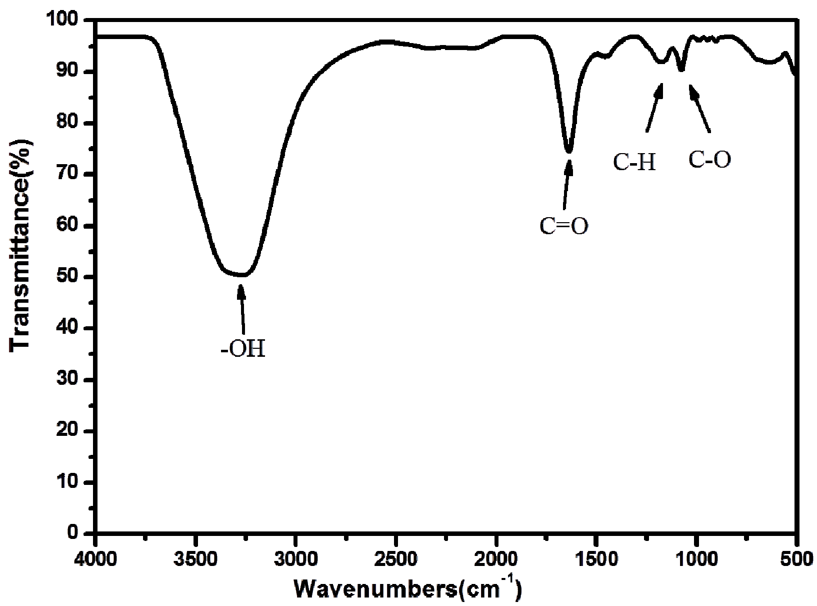

Figure S1. FTIR spectra of the CQDs.

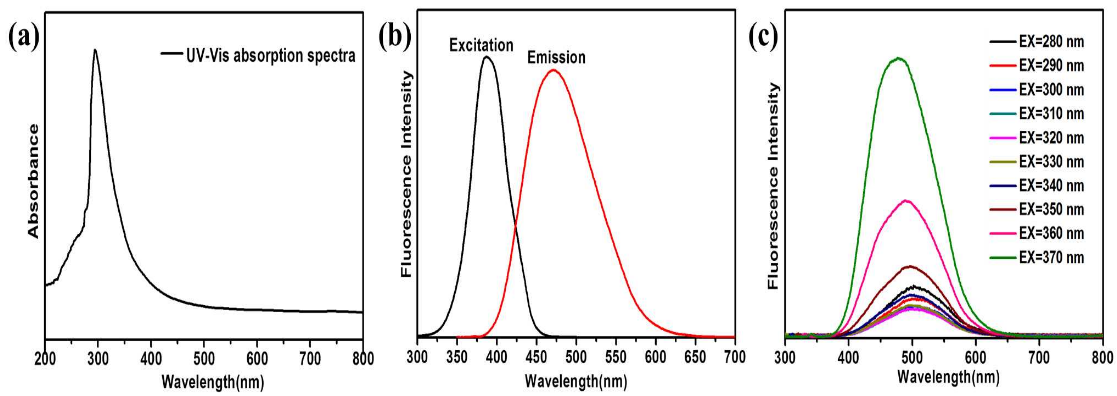

Figure S2. (a) UV-Vis absorption of CQDs, (b) the maximum excitation spectrum and emission spectrum of CQDs, (c) emission spectrum of CQDs at different excitation wavelengths.

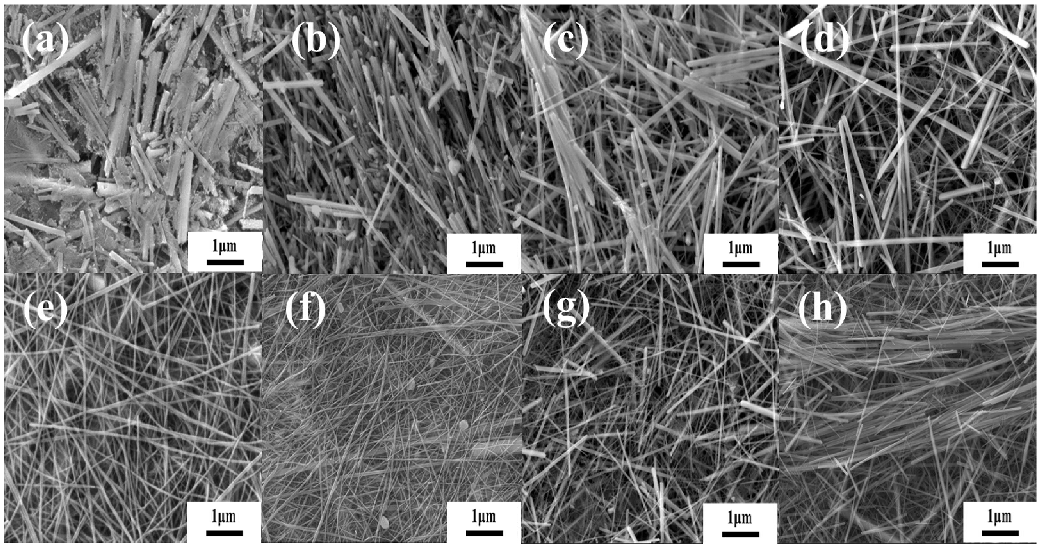

Figure S3. SEM images of the composite films with different reaction time. (a-h) the reaction time of the composite films are 2、4、6、8、10、12、14、16 h.

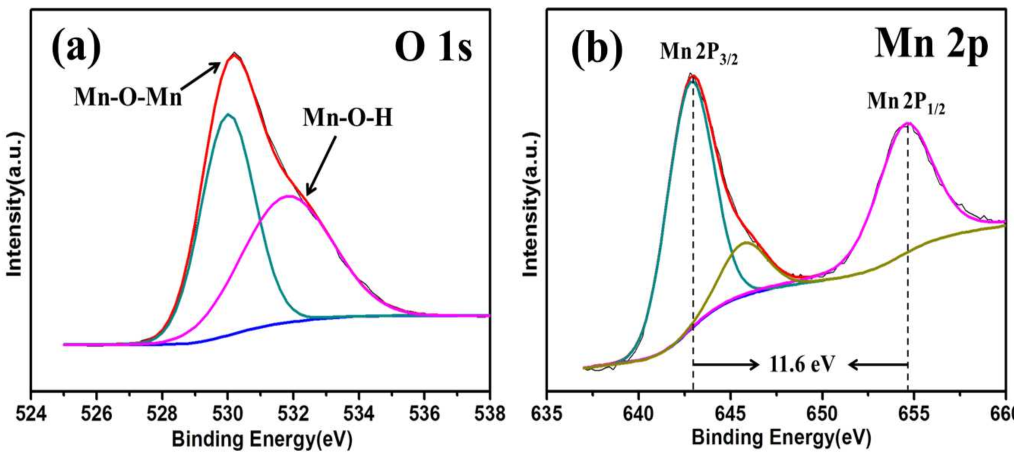

Figure S4. High-resolution XPS curves of (a) O1s, (b) Mn2p for the MnO_2 nanorods.

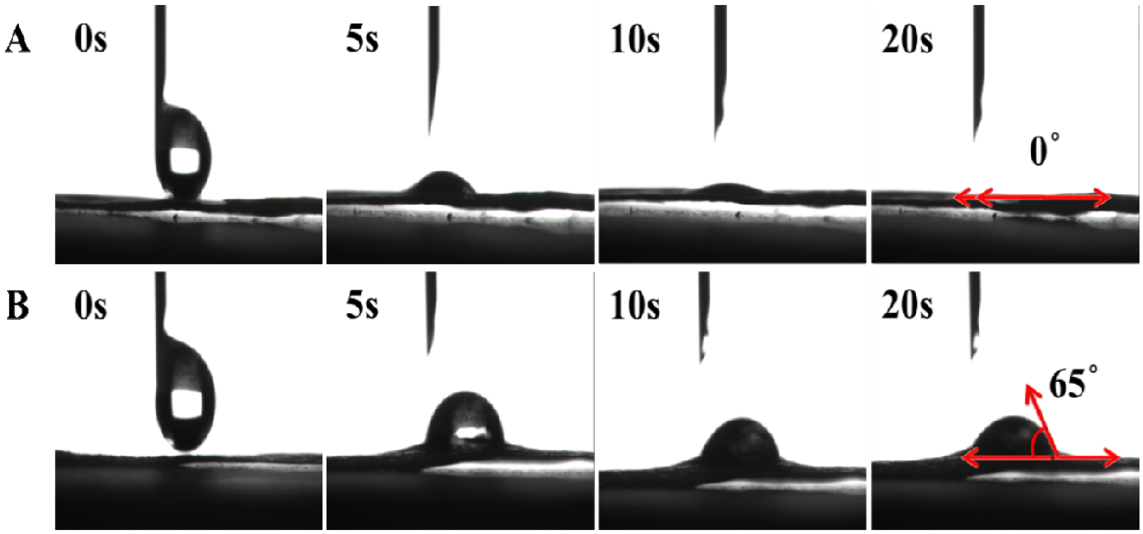

Figure S5. Photographs of the water droplet shape on the samples (A the film of MnO_2/CQDs nanowires, B the film of MnO_2 nanorods) at 0、5、10、20 s. Insert shows contact angle at the end of process.

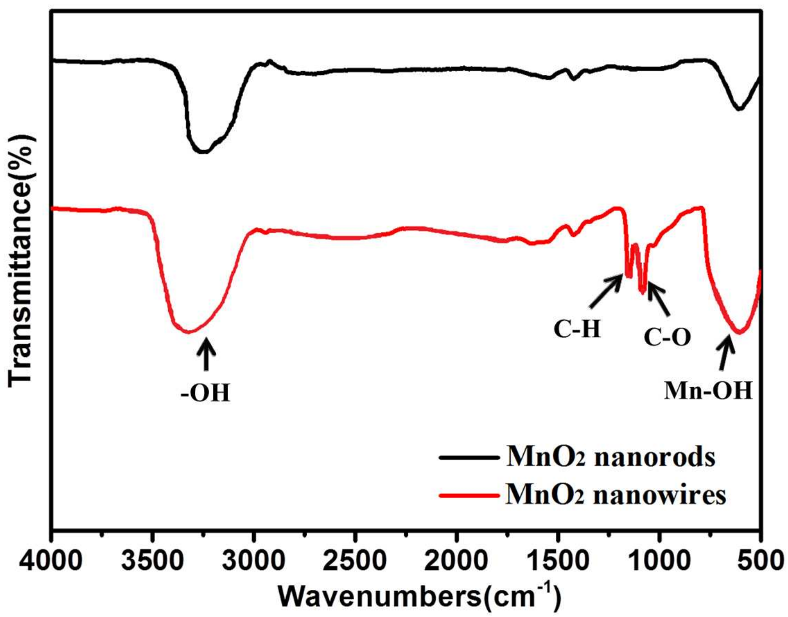

Figure S6. FTIR spectra of the MnO_2 nanorods and the CQDs-induced MnO_2 nanowires.

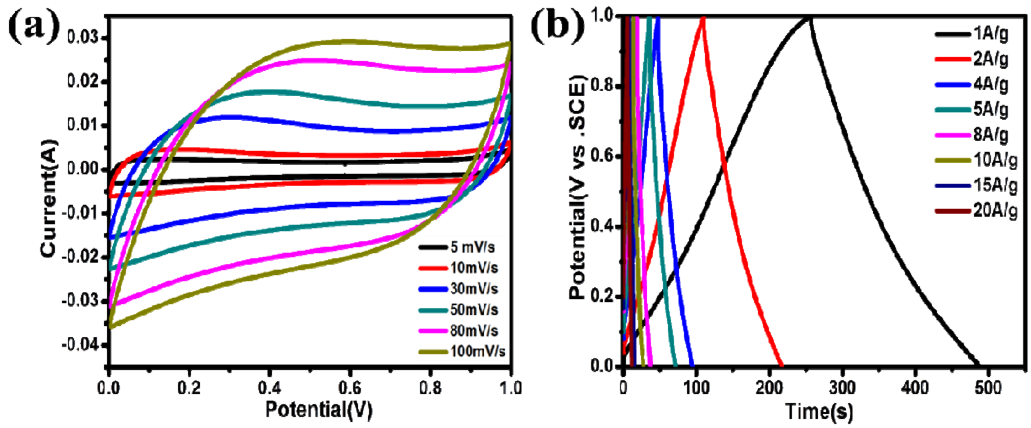

Figure S7. Electrochemical performance of the MnO_2 nanorods measured in a three-electrode system. (a) CV curves at different scan rate from 5 to 100 m Vs^{-1}. (b) GCD curves at different current densities from 1 to 20 A g^{-1}.

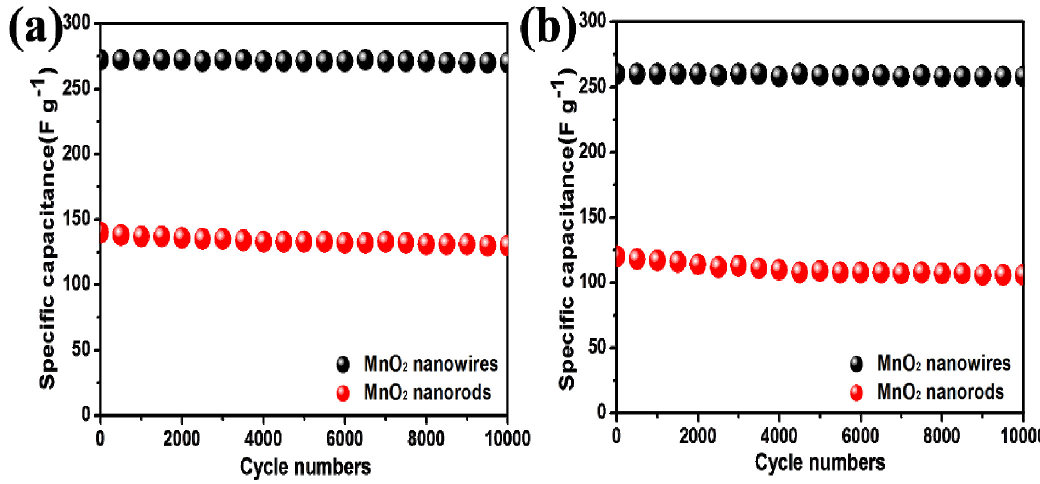

Figure S8. Cyclic stability of the MnO_2/CQDs nanowires and MnO_2 nanorods measured in a three-electrode system at (a) 10 A g^{-1} and (b) 20 A g^{-1}.

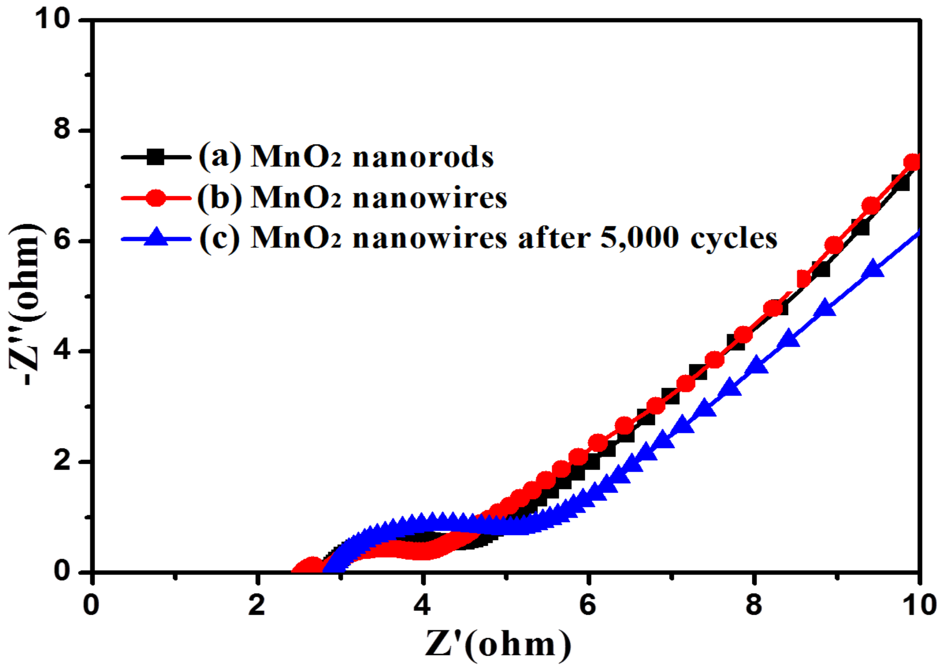

Figure S9. Nyquist plot of (a) MnO_2 nanorods; (b) MnO_2 nanowires; (c) MnO_2 nanowires after 5,000 cycles at 10A g^{-1}

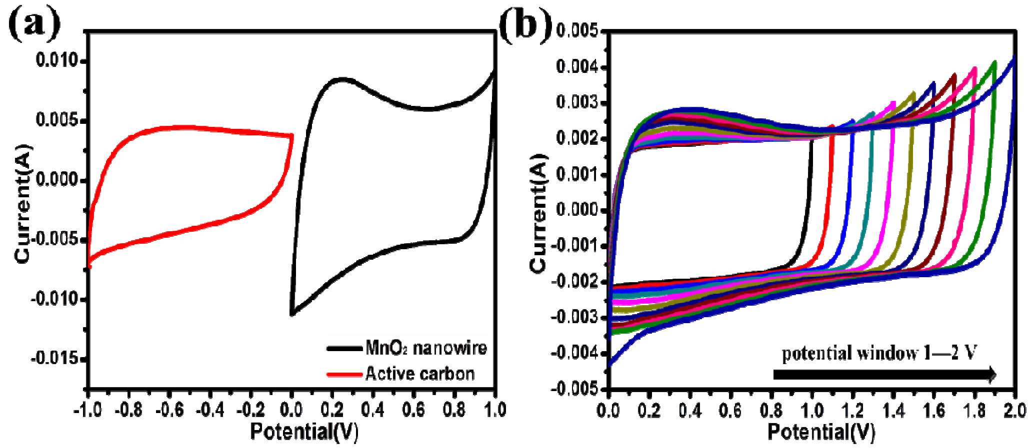

Figure S10. CV curves of (a) MnO_2/CQDs nanowire and active carbon at 10 m Vs^{-1} and (b) the asymmetric capacitor with potential windows range from 1 to 2V.

Table S1. Comparison of electrochemical performance of different MnO_2 materials

Electrodes	Specific capacity ($mAh\ g^{-1}$)	Cycle numbers	Capacitance retention (%)	Reference
MnO_2/CQDs NW	340F g^{-1}at 1A g^{-1} 260F g^{-1} at 20 A g^{-1}	10000	80.1%	This work
Porous MnO_2	218F g^{-1} at 1A g^{-1} 153F g^{-1} at 15A g^{-1}	4000	90%	S1
Cage-like MnO_2 -Mn_2O_3 hollow spheres	239.8F g^{-1} at 1m V s^{-1}	2000	77.4%	S2
δ-MnO_2 holey graphene	245F g^{-1} at 1 A g^{-1}	1000	81%	S3
MnO_2/Graphene	267F g^{-1} at 0.2 A g^{-1}	7000	72%	S4
MnO_2	308 F g^{-1} at 0.2 A g^{-1}	3000	91%	S5

References

(S1) Xie, X.; Zhang, C.; Wu, M. B.; Tao, Y.; Lv, W.; Yang, Q. Porous MnO_2 for Use in a High Performance Supercapacitor: Replication of a 3D Graphene Network as a Reactive Template. *Chem. commun.* **2013**, *49*, 11092-11094.

(S2) Ji, S.; Ma, Y.; Wang, H.; Key, J.; Brett, D. J. L.; Wang, R. Cage-Like MnO_2-Mn_2O_3 Hollow Spheres with High Specific Capacitance and High Rate Capability as Supercapacitor Material. *Electrochim. Acta*, 2016, 219, 540-546.

(S3) Zhang, J.; Yang, X.; He, Y.; Bai, Y.; Kang, L.; Xu, H.; Shi, F.; Lei, Z.; Liu, Z. δ-MnO_2/Holey Graphene Hybrid Fiber for All-Solid-State Supercapacitor. *J. Mater. Chem. A* **2016**, *4*, 9088-9096.

(S4) Peng, L.; Peng, X.; Liu, B.; Wu, C.; Xie, Y.; Yu, G. Ultrathin Two-Dimensional MnO_2/Graphene Hybrid Nanostructures for High-Performance, Flexible Planar Supercapacitors. *Nano Lett* **2013**, *13*, 2151-2157.

(S5) Gao, L.; Zhang, L.; Jia, S.; Liu, X.; Wang, Y.; Xing, S. Facile Route to Achieve Hierarchical Hollow MnO_2 Nanostructures. *Electrochim. Acta* **2016**, *203*, 59-65.